TRIM21 silencing inhibits the apoptosis and expedites the osteogenic differentiation of dexamethasone-induced MC3T3-E1 cells by activating the Keap1/Nrf2 pathway

JIAQI SHI, LI CHEN, XU WANG and XIN MA

Department of Orthopedics, Huashan Hospital Affiliated to Fudan University, Shanghai 200040, P.R. China

Received November 16, 2023; Accepted February 13, 2024

DOI: 10.3892/etm.2024.12502

Abstract. Steroid-induced osteonecrosis of the femoral head (ONFH) is a serious complication caused by long-term or excessive use of glucocorticoids. The present study aimed to ascertain the effects of tripartite motif-containing protein 21 (TRIM21) on the process of steroid-induced ONFH and its hidden action mechanism. TRIM21 expression in dexamethasone (Dex)-treated mouse MC3T3-E1 preosteoblast cells was examined using reverse transcription-quantitative PCR and western blotting. The Cell Counting Kit-8 (CCK-8) method and lactate dehydrogenase release assay were used to respectively measure cell viability and injury. Flow cytometry analysis was used to assay cell apoptosis. Caspase 3 activity was evaluated using a specific assay, while alkaline phosphatase and Alizarin red S staining were used to evaluate osteogenesis. 2,7-dichloro-dihydrofluorescein diacetate fluorescence probe was used to estimate reactive oxygen species generation. Specific assay kits were used to appraise oxidative stress levels. In addition, the expression of apoptosis-, osteogenic differentiation- and Kelch-like ECH-associated protein 1 (Keap1)/nuclear factor erythroid 2-related factor 2 (Nrf2) signaling-associated proteins was assessed using western blotting. In Nrf2 inhibitor (ML385)-pretreated MC3T3-E1 cells exposed to Dex, cell apoptosis, osteogenesis and oxidative stress were detected again as aforementioned. Results revealed that TRIM21 expression was raised in Dex-induced MC3T3-E1 cells and TRIM21 deletion improved the viability and osteogenic differentiation, whereas it hampered the oxidative stress and apoptosis in MC3T3-E1 cells with Dex induction. In addition, silencing of TRIM21 activated Keap1/Nrf2 signaling. Moreover, ML385 partially abrogated the effects of TRIM21 depletion on the oxidative stress, apoptosis and osteogenic differentiation in MC3T3-E1 cells exposed to Dex. In conclusion, TRIM21 silencing might activate Keap1/Nrf2 signaling to protect against steroid-induced ONFH.

Correspondence to: Dr Xin Ma, Department of Orthopedics, Huashan Hospital Affiliated to Fudan University, 12 Urumqi Middle Road, Jing'an, Shanghai 200040, P.R. China
E-mail: xinma2762@163.com

Key words: steroid-induced osteonecrosis of the femoral head, tripartite motif-containing protein 21, osteogenic differentiation, Kelch-like ECH-associated protein 1/nuclear factor erythroid 2-related factor 2 signaling, oxidative stress

Introduction

Steroid-induced osteonecrosis of the femoral head (ONFH), a serious orthopedic disease caused by long-term or excessive use of glucocorticoids, is a bone disorder primarily presenting femoral head collapse, resulting in hip joint dysfunction and eventually total hip arthroplasty (1,2). The prevalence rate of ONFH in Japan is ~0.0182%, while in South Korea it is ~0.0289% (3). Considering that, there is a pressing need to understand the specific molecular mechanism behind ONFH and ascertain potential therapeutic biomarkers.

The tripartite motif (TRIM) family of proteins belonging to the subfamily of E3 ubiquitin ligases has been shown to be implicated in diversified human diseases, such as tumors, inflammatory, infectious, neuropsychiatric disorders, chromosomal abnormalities as well as developmental diseases (4). As a member of the TRIM family, tripartite motif-containing protein 21 (TRIM21) can function as an E3 ligase dependent on its RING domain (5). Initially, TRIM21 was identified to act as a regulator of immune responses and participate in autoimmune diseases (5-7). A recent study revealed that TRIM21 has low expression during the osteogenic process of mesenchymal stem cells and TRIM21 negatively regulates the osteogenic capacity of mesenchymal stem cells both *in vitro* and *in vivo* (8). Nevertheless, the effects of TRIM21 on the process of ONFH remain to be elucidated.

Nuclear factor erythroid 2-related factor 2 (Nrf2) which is modulated by Kelch-like Ech-associated protein-1 (Keap1) is regarded as a principal component of the cellular defense system responding to various types of endogenous and exogenous insults (9). Numerous studies showed that the Keap1/Nrf2 pathway participates in a multitude of biological events including metabolism, cell proliferation and cell death (10,11). Notably, dysregulation of the Nrf2/Keap1 pathway has been shown to be involved in the process of ONFH (12). Concurrently, TRIM21 was reported to block the Keap1/Nrf2 pathway in hepatocarcinogenesis (13).

The present study sought to unravel the regulatory role of TRIM21 in the development of steroid-induced ONFH and to

identify whether its action mechanism was associated with the Keap1/Nrf2 pathway.

Materials and methods

Cell culture and treatment. Minimal essential medium α (MEMα; Corning, Inc.) supplemented with 10% fetal bovine serum (FBS; Wuhan Saios Biotechnology Co., Ltd.) was adopted for the incubation of murine preosteoblast MC3T3-E1 (Wuhan Saios Biotechnology Co., Ltd.) cells at 37˚C with 5% CO_2. Dexamethasone (Dex; Shanghai Macklin Biochemical Co., Ltd.) at the concentration of 1 μM was used to treat MC3T3-E1 cells for 24 h at 37˚C (14). Additionally, cells were treated with 10 μM Nrf2 inhibitor ML385 (Shanghai Macklin Biochemical Co., Ltd.) for 24 h at 37˚C (15) before treatment with Dex. To stimulate osteogenic differentiation, the osteogenesis-inducing medium containing 10% FBS, 5 mM L-glycerophosphate, 100 nM Dex and 50 mg/ml ascorbic acid was applied to the culture of MC3T3-E1 cells at 80% confluence and incubated for 7 days at 37˚C.

Transfection protocol. MC3T3-E1 cells at the logarithmic phase were seeded in a 6-well plate ($1x10^5$ cells/well) and were incubated at 37˚C until they reached 80% confluence. Using Lipofectamine® 3000 (Invitrogen; Thermo Fisher Scientific, Inc.), MC3T3-E1 cells were established with a stable knockdown of TRIM21 using 50 nmol/l short hairpin RNAs (shRNAs) for TRIM21 (sh-TRIM21#1, sense 5'-GAACCTGGACACGTTAGATAT-3', antisense 5'-ATATCTAACGTGTCCAGGTTC-3'; sh-TRIM21#2, sense 5'-TTGTCTCCTTCTACAACATAA-3', antisense 5'-TTATGTTGTAGAAGGAGACAA-3') or 50 nmol/l control shRNA (sh-NC, sense 5'-TACGGAGGACTCGATCTAG-3', antisense 5'-CTAGATCGAGTCCTCCGTA-3') ordered from Shanghai GenePharma Co., Ltd., according to the manufacturer's protocol at 37˚C for 48 h. Following 48 h of culture at 37˚C, cells were harvested for the subsequent experiments.

Cell Counting Kit-8 (CCK-8) assay. MC3T3-E1 cells subjected to transfection and indicated treatment were plated into 96-well plates (3,000 cells/well). After being incubated for 2 h with 10 μl CCK-8 solution (Beyotime Institute of Technology), the absorbance was recorded at 450 nm by using a microplate reader (BMG-Labtech, Ltd.).

Lactate dehydrogenase (LDH) release assay. The cytotoxicity in the supernatants of MC3T3-E1 cells subjected to centrifugation at 8,000 x g for 10 min at 4˚C was examined with an LDH assay kit (Nanjing Jiancheng Bioengineering Institute). Absorbance was reco.

Evaluation of reactive oxygen species (ROS) production. A 2 μM 2,7-dichloro-dihydrofluorescein diacetate (DCFH-DA; Shanghai Aladdin Biochemical Technology Co., Ltd.) solution was added to the MC3T3-E1 cells, previously subject to transfection and indicated treatment, for 30 min of incubation at 37˚C in the dark. Following washing with PBS, the fluorescence intensity was observed under a fluorescence microscope (Zeiss GmbH).

Detection of oxidative stress indexes. Following centrifugation at 8,000 x g for 10 min at 4˚C, superoxide dismutase (SOD; cat. no. S930985), glutathione peroxidase (GSH-Px; cat. no. G930918) and malonaldehyde (MDA; cat. no. M930417) contents were evaluated using specific assay kits from Shanghai Macklin Biochemical Co., Ltd. The absorbance values were recorded using a microplate reader.

Flow cytometry analysis. An Annexin V-fluorescein isothiocyanate (FITC) apoptosis detection kit (Nanjing KeyGen Biotech Co., Ltd.) was used to assess the apoptosis of MC3T3-E1 cells subjected to transfection and indicated treatment. Cells were plated into 6-well plates and incubated at 37˚C. MC3T3-E1 cells were suspended in the binding buffer containing Annexin-V-FITC and PI. The apoptosis rate was detected using flow cytometry (BD FACSCalibur; BD Biosciences). Data were analyzed using FlowJo software v7.6.1 (Tree Star, Inc.). The apoptotic rate was calculated as the percentage of early + late apoptotic cells.

Measurement of caspase 3 activity. Caspase 3 activity was examined with a caspase-3 activity assay kit (cat. no. ab252897; Abcam) according to the manufacturer's instructions. Cell lysates were incubated with caspase-3 substrate DEVD-AFC for 2 h at 37˚C in the dark. The fluorescence was observed using a fluorescence plate reader (excitation at 400 nm and emission at 505 nm).

Alkaline phosphatase (ALP) staining and Alizarin red S (ARS) staining. Following osteogenic differentiation, MC3T3-E1 cells previously subjected to transfection and indicated treatment were fixed in 4% paraformaldehyde for 15 min at 37˚C, before being incubated with ALP staining solution (MK BioScience Co., Inc.) for 4 h or ARS solution (Shanghai Macklin Biochemical Co., Ltd.) for 30 min at 37˚C. The images were captured under an inverted light microscope (Zeiss GmbH).

Reverse transcription-quantitative (RT-q) PCR. Extraction of total RNA from $1x10^4$ MC3T3-E1 cells was conducted using TRIzol® reagent (Thermo Fisher Scientific, Inc.). The cDNA was synthesized using the PrimeScript RT reagent kit (Takara Bio, Inc.) according to the instructions provided by the manufacturer. qPCR was performed on the ABI 7500 Real-Time PCR system (Applied Biosystems; Thermo Fisher Scientific, Inc.) with cDNA as templates using SYBR Green PCR Master Mix Reagents (Takara Bio, Inc.) according to the manufacturer's instructions. The following thermocycling conditions were used for qPCR: Initial denaturation for 2 min at 94˚C; followed by 35 cycles for 30 sec at 94˚C and 45 sec at 55˚C. The calculation of relative mRNA levels was performed based on the $2^{-\Delta\Delta Cq}$ method (16). GAPDH was employed as the internal reference. Specific primer sequences were: TRIM21 forward, 5'-CCTGGTTAGATTCCACGGCA-3' and reverse, 5'-TGAACTGCCCCCATTCTTCC-3'; and GAPDH forward, 5'-GCCTCCTCCAATTCAACCCT-3' and reverse, 5'-CTCGTGGTTCACACCCATCA-3'. All experiments were replicated three times.

Western blotting. After the preparation of cellular lysates using RIPA buffer (Beyotime Institute of Biotechnology), the

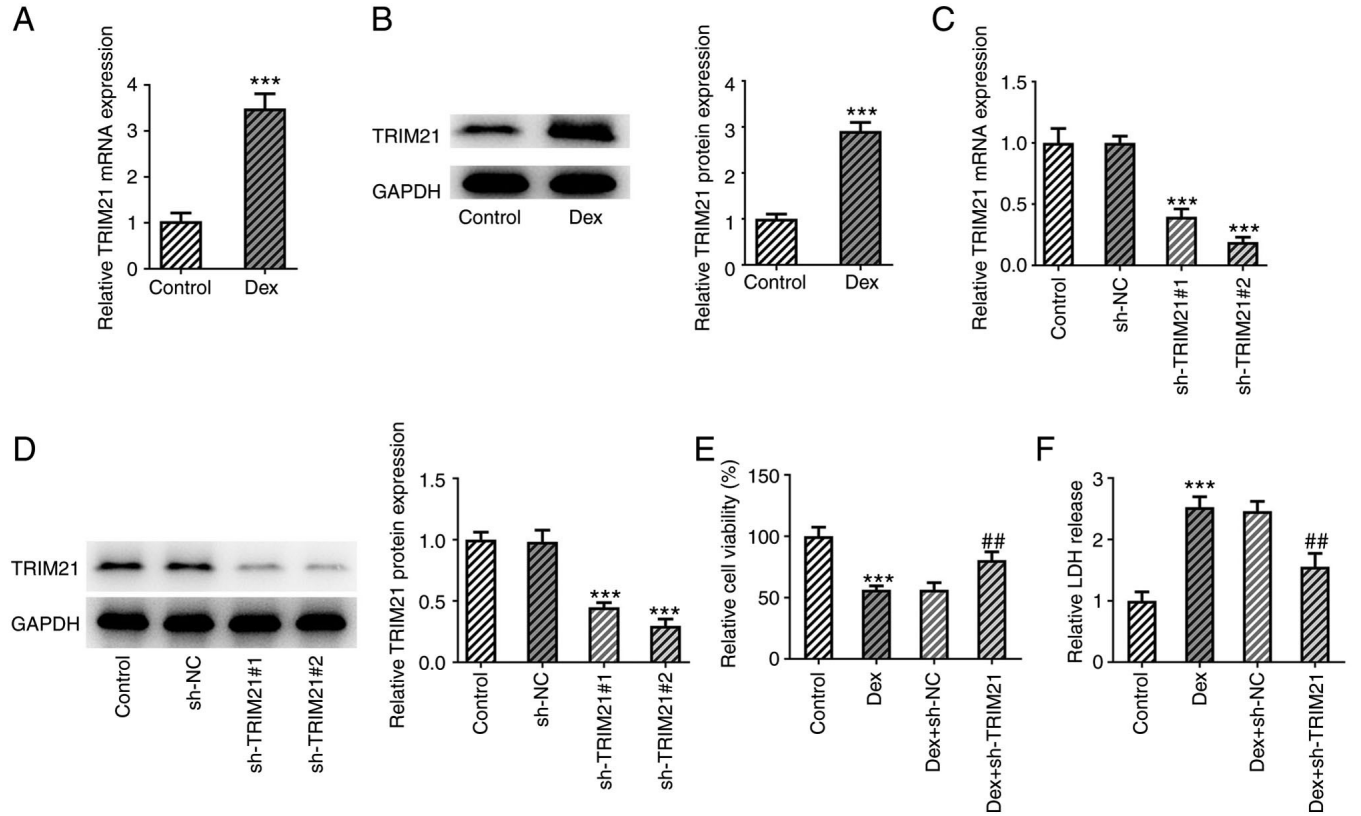

Figure 1. Interference with TRIM21 raises the viability and reduces the cytotoxicity in Dex-treated MC3T3-E1 cells. (A) RT-qPCR and (B) western blotting of TRIM21 expression. ***P<0.001 vs. control group. (C) RT-qPCR and (D) western blotting tested the transfection efficacy of sh-TRIM21#1 and sh-TRIM21#2. ***P<0.001 vs. sh-NC group. (E) Cell viability was assayed by the CCK-8 method. (F) An LDH assay kit examined LDH release. ***P<0.001 vs. control group; ##P<0.01 vs. Dex + sh-NC group. TRIM21, tripartite motif-containing protein 21; Dex, dexamethasone; RT-qPCR, reverse transcription-quantitative PCR; sh, short hairpin RNA; sh-TRIM21; sh-RNA targeting TRIM21; sh-NC, sh-RNA negative control; LHD, lactate dehydrogenase.

quantification of protein concentration was performed using the BCA method (Beyotime Institute of Biotechnology). Total protein (40 μg protein per lane) was separated on 10% gels using SDS-PAGE and then transferred onto the polyvinylidene difluoride membranes. After blocking with 5% BSA (Beyotime Institute of Biotechnology) for 1.5 h at room temperature, the membranes were then immunoblotted with primary antibodies including TRIM21 (cat. no. ab207728; 1:1,000; Abcam), B-cell lymphoma 2 (Bcl-2; cat. no. ab196495; 1:2,000; Abcam), Bcl-2 associated X (Bax; cat. no. ab3191; 1:1,000; Abcam), osterix (Osx; cat. no. ab209484; 1:1,000; Abcam), runt-related transcription factor 2 (RUNX2; cat. no. ab236639; 1:1,000; Abcam), bone morphogenetic protein 2 (BMP2; cat. no. ab284387; 1:1,000; Abcam), Nrf2 (cat. no. 12721; 1:1,000; Cell Signaling Technology, Inc.), Keap1 (cat. no. ab119403; 1:1,000; Abcam), heme oxygenase-1 (HO-1; cat. no. ab189491; 1:2,000; Abcam), NAD(P)H:quinone oxidoreductase 1 (NQO1; cat. no. ab80588; 1:10,000; Abcam) and GAPDH (cat. no. ab181603; 1:10,000; Abcam) at 4˚C overnight, before being probed with HRP-conjugated secondary antibody (cat. no. ab6721; 1:2,000; Abcam) for 1 h at room temperature. Protein signals were visualized using chemiluminescence reagents (MilliporeSigma). The western blotting images of proteins were processed using ImageJ software (version 1.8.0; National Institutes of Health) with GAPDH as the loading control.

Statistical analysis. Data are presented as mean ± standard deviation of three independent experiments and analyzed using GraphPad Prism 8 software (GraphPad Software, Inc.; Dotmatics). Statistical comparison between two groups was made using an unpaired student's t-test. One-way analysis of variance followed by Tukey's post hoc test was used to compare the effects of more than two groups. P<0.05 was considered to indicate a statistically significant difference.

Results

TRIM21 knockdown increases viability and reduces cytotoxicity in Dex-treated MC3T3-E1 cells. To investigate the role of TRIM21 in ONFH, Dex was initially used for the establishment of a cell model of ONFH in MC3T3-E1 cells. Subsequently, TRIM21 mRNA levels and protein expression were evaluated using RT-qPCR and western blotting, respectively, and TRIM21 expression was noticeably increased in MC3T3-E1 cells administered with Dex (Fig. 1A and B). Moreover, TRIM21 expression was distinctly decreased after transfection of sh-TRIM21#1/2 (Fig. 1C and D). Therefore, sh-TRIM21#2 was chosen for the follow-up assays as TRIM21 exhibited lower expression in the sh-TRIM21#2 group. Based on the data from the CCK-8 assay, the viability was diminished in MC3T3-E1 cells exposed to Dex and the viability of Dex-treated MC3T3-E1 cells was improved through the knockdown of TRIM21 (Fig. 1E). In addition, the results

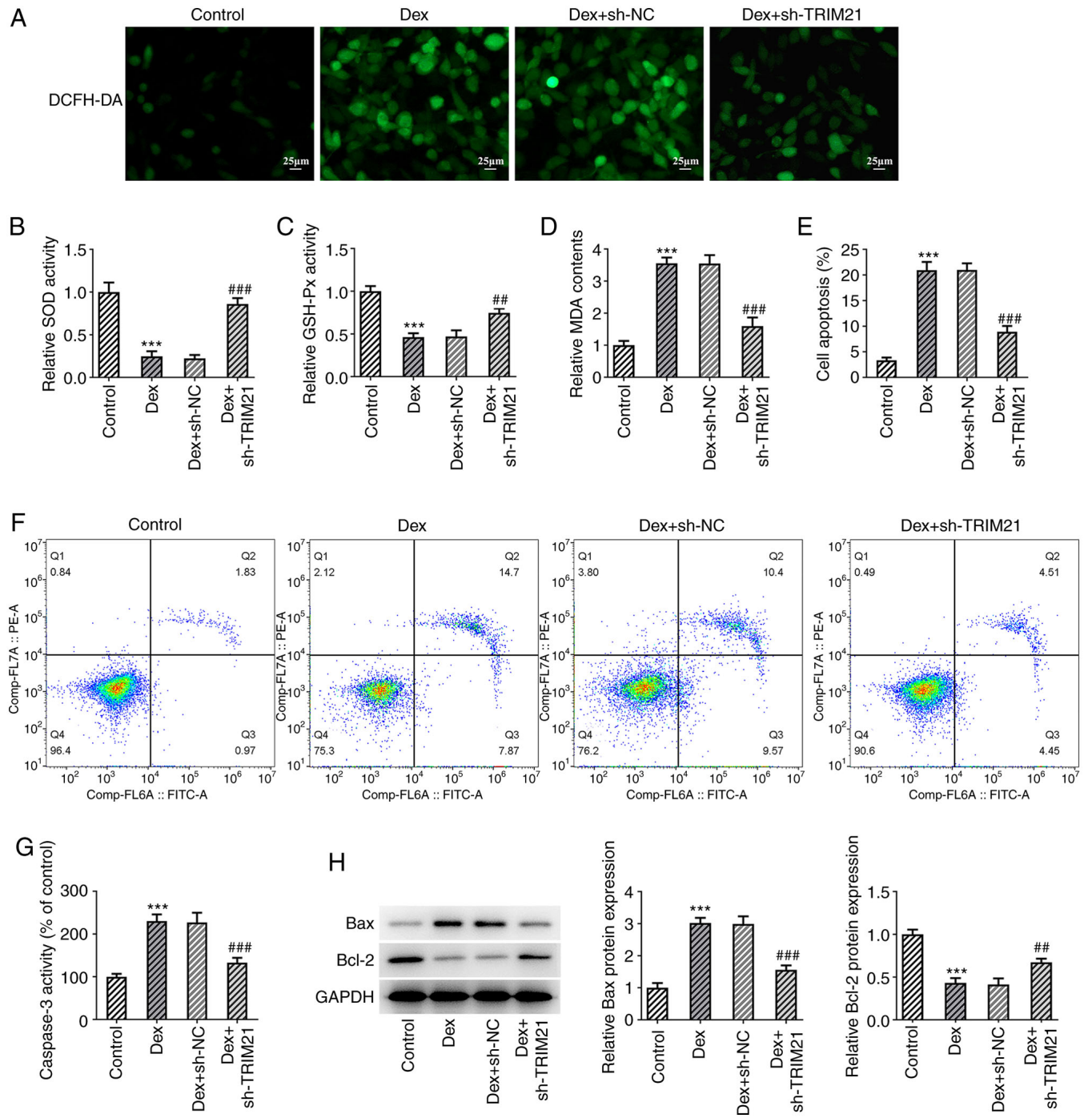

Figure 2. Interference with TRIM21 mitigates oxidative stress and apoptosis of Dex-challenged MC3T3-E1 cells. (A) DCFH-DA staining evaluated ROS generation. The levels of (B) SOD, (C) GSH-Px and (D) MDA were detected using the corresponding kits. (E and F) Flow cytometry analysis of cell apoptosis. (G) Caspase 3 activity as measured by a kit. (H) Western blotting tested the expression of apoptosis-associated proteins. ***P<0.001 vs. control group; $^{##}$P<0.01, $^{###}$P<0.001 vs. Dex + sh-NC group. TRIM21, tripartite motif-containing protein 21; Dex, dexamethasone; DCFH-DA, 2,7-dichloro-dihydrofluorescein diacetate; ROS, reactive oxygen species; SOD, superoxide dismutase; GSH-Px, glutathione peroxidase; MDA, malonaldehyde; sh-, short hairpin RNA; sh-NC, sh-RNA negative control.

from the LDH assay showed that the stimulated LDH release in Dex-challenged MC3T3-E1 cells was decreased when TRIM21 was silenced (Fig. 1F). In conclusion, TRIM21 knockdown suppressed Dex-stimulated viability loss and LDH release in MC3T3-E1 cells.

TRIM21 knockdown mitigates oxidative stress and apoptosis of Dex-challenged MC3T3-E1 cells. At the same time, as elucidated using DCFH-DA staining, TRIM21 silencing decreased Dex-induced ROS production in MC3T3-E1 cells (Fig. 2A). Dex exposure diminished SOD and GSH-Px activities whilst upregulating MDA content in MC3T3-E1 cells, which were all partially reversed by silencing of TRIM21 (Fig. 2B-D). The apoptosis of MC3T3-E1 cells was evaluated upon exposure to Dex. As shown in Fig. 2E and F, Dex treatment markedly increased the apoptotic rate of MC3T3-E1 cells,

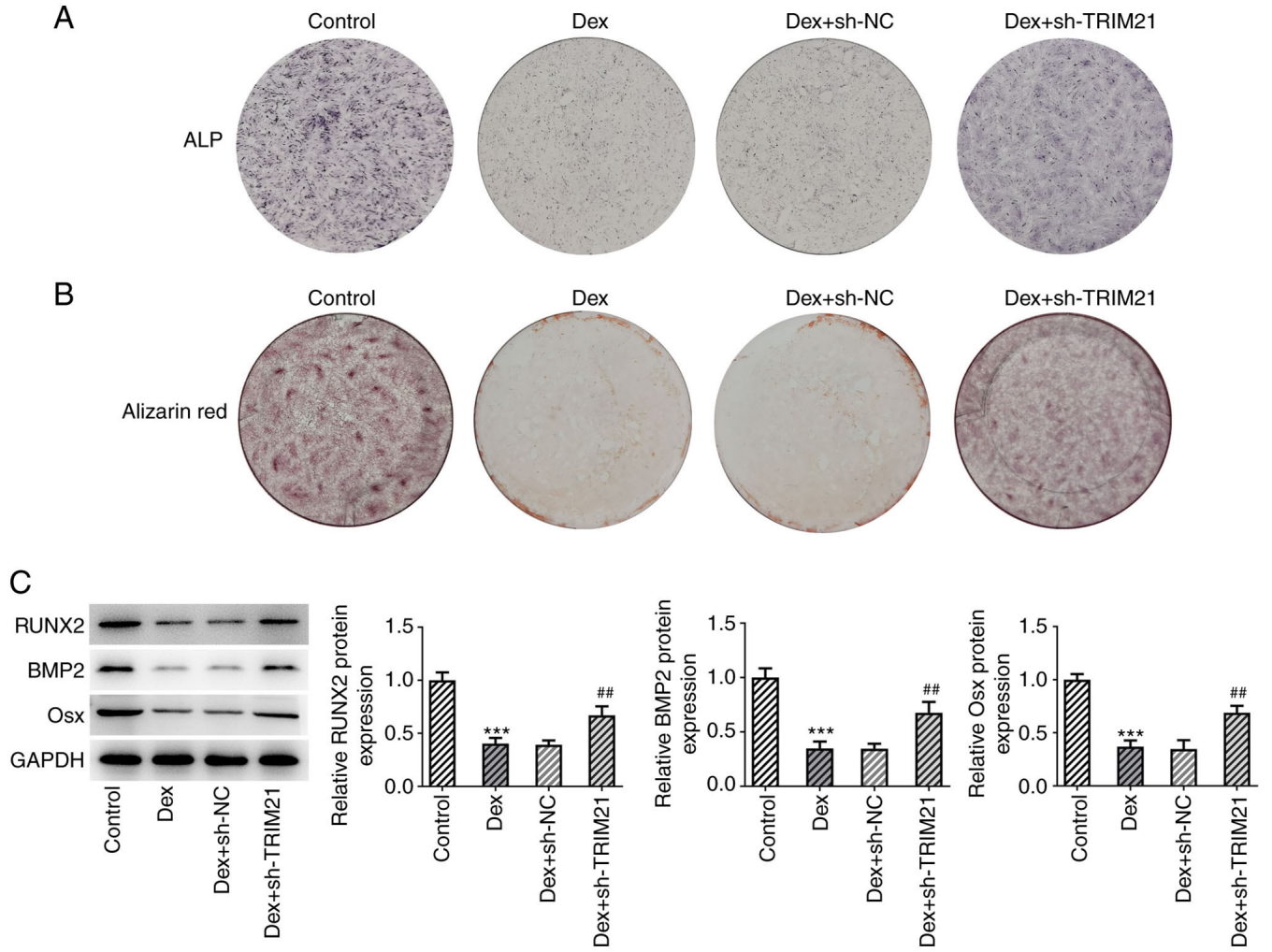

Figure 3. Interference with TRIM21 contributes to the osteogenic differentiation of MC3T3-E1 cells exposed to Dex. (A) ALP staining measured ALP activity. (B) Alizarin red S staining estimated calcium salt deposition. (C) Western blotting tested the expression of osteogenic differentiation-associated proteins. ***P<0.001 vs. control group; ##P<0.01 vs. Dex + sh-NC group. TRIM21, tripartite motif-containing protein 21; Dex, dexamethasone; ALP, alkaline phosphatase; RUNX2, runt-related transcription factor 2; BMP2, bone morphogenetic protein 2; Osx, osterix; sh-, short hairpin RNA; sh-NC, sh-RNA negative control.

which was then decreased following TRIM21 knockdown. The increased caspase 3 activity that was found in MC3T3-E1 cells challenged with Dex was decreased when TRIM21 was knocked down (Fig. 2G). Western blotting also implied that Dex treatment resulted in the upregulation of Bax expression and the downregulation of Bcl-2 expression in MC3T3-E1 cells (Fig. 2H). However, in MC3T3-E1 cells treated with Dex, transfection of sh-TRIM21#2 clearly reduced Bax expression although is strengthened Bcl-2 expression. Overall, TRIM21 knockdown impeded Dex-stimulated oxidative stress and apoptosis in MC3T3-E1 cells.

Interference with TRIM21 contributes to the osteogenic differentiation of MC3T3-E1 cells exposed to Dex. Using ALP staining, it was observed that the decreased ALP activity in MC3T3-E1 cells treated with Dex increased again following TRIM21 knockdown (Fig. 3A). Furthermore, the data from the ARS staining showed that the attenuated calcium accumulation in MC3T3-E1 cells caused by Dex treatment was aggravated by the TRIM21 knockdown (Fig. 3B). Western blotting analysis of osteogenic differentiation-related markers also indicated that Dex exposure decreased Osx, RUNX2 and BMP2 protein expressions in MC3T3-E1 cells, which were partly restored following knockdown of TRIM21 (Fig. 3C). In summary, TRIM21 knockdown exacerbated the differentiation of Dex-treated MC3T3-E1 cells into osteoblasts.

TRIM21 knockdown activates the anti-oxidant Keap1/Nrf2 pathway. The expression of Keap1/Nrf2 pathway-related proteins was investigated by the present study because the Keap1/Nrf2 pathway was shown to play an inhibitory role in oxidative stress (17). The decreased Nrf2, HO-1 and NQO1 expression and the increased Keap1 expression in Dex-challenged MC3T3-E1 cells were all restored after TRIM21 was knocked down (Fig. 4), suggesting that TRIM21 inhibition might activate Keap1/Nrf2 signaling in Dex-induced MC3T3-E1 cells.

TRIM21 knockdown activates Keap1/Nrf2 signaling to hamper the oxidative stress and apoptosis and drives the osteogenic differentiation in Dex-treated MC3T3-E1 cells. The present study employed the Nrf2 inhibitor ML385 to test the hypothesis that TRIM21 might participate in the biological events in the Dex-induced cellular model of ONFH

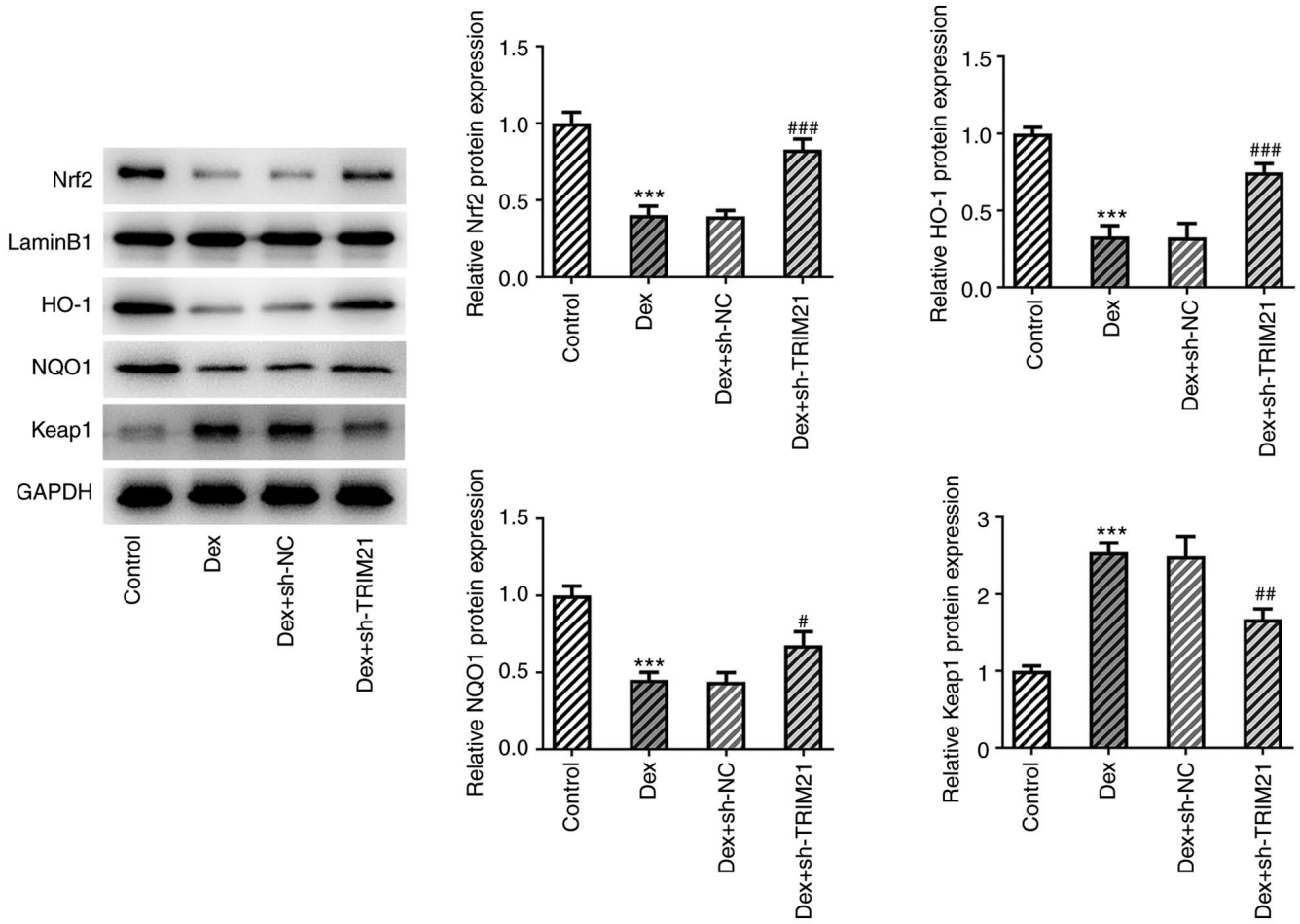

Figure 4. TRIM21 deficiency activates the anti-oxidant Keap1/Nrf2 pathway. Western blotting was used to examine the expression of proteins involved in the Keap1/Nrf2 pathway. ***P<0.001 vs. control group; $^{\#}$P<0.05, $^{\#\#}$P<0.01, $^{\#\#\#}$P<0.001 vs. Dex + sh-NC group. TRIM21, tripartite motif-containing protein 21; Keap1, Kelch-like ECH-associated protein 1; Nrf2, nuclear factor erythroid 2-related factor 2; HO-1, heme oxygenase-1; NQO1, NAD(P)H:quinone oxidoreductase 1; sh-, short hairpin RNA; sh-NC, sh-RNA negative control; Dex, dexamethasone.

by mediating Keap1/Nrf2 signaling. Compared with the Dex group, ROS and MDA levels were decreased whilst SOD and GSH-Px activities were increased in Dex + sh-TRIM21 group (Fig. 5A-D). However, ROS (detected by DCFH-DA staining) and MDA levels were upregulated while SOD and GSH-Px activities were downregulated in the Dex + sh-TRIM21 + ML385 group compared with the Dex + sh-TRIM21 group. In addition, the weakened apoptotic rate, accompanied by the declined caspase 3 activity, Bax expression and elevated Bcl-2 expression in Dex-exposed MC3T3-E1 cells transfected with TRIM21 shRNA were all partially counteracted by pretreatment with ML385 (Fig. 5E-H). Additionally, TRIM21 deletion improved ALP activity and calcium accumulation in MC3T3-E1 cells challenged with Dex, which were then partially abrogated by ML385, implying that the stimulatory role of TRIM21 knockdown in the osteogenic differentiation of Dex-exposed MC3T3-E1 cells was abolished by inactivation of Nrf2 (Fig. 6A and B). This finding was also evidenced by the decreased Osx, RUNX2 and BMP2 expressions in Dex + sh-TRIM21 + ML385 group compared with the Dex + sh-TRIM21 group (Fig. 6C). In conclusion, inhibition of Nrf2 partly counteracted the effects of TRIM21 knockdown on the oxidative stress, apoptosis and osteogenic differentiation in Dex-treated MC3T3-E1 cells.

Discussion

Osteoblasts, which are the sole bone-forming cells, are responsible for bone formation and maintenance of bone mass. Osteoblast dysfunction is one of the pivotal mechanisms leading to steroid-induced ONFH (18) and autologous osteoblast cell implantation may be regarded as an effective therapy for ONFH (19). Administration with glucocorticoids, extensively applied for the treatment of autoimmune and inflammatory diseases as immunosuppressive and anti-inflammatory drugs, is the most common non-traumatic cause of ONFH (20). As an artificially synthetic glucocorticoid, Dex has also been implicated in the process of ONFH. In particular, Dex has been proposed to suppress the differentiation and stimulate apoptosis, autophagy, ferroptosis and oxidative stress in osteoblasts (21-23). Osteoblast cells caused by stimulation with 1 μM Dex for 24 h have been widely used as a cell model to explore the mechanisms involving in steroid-related ONFH (14,24,25). Thus, the mechanism underlying Dex-induced ONFH was investigated in the present study after murine MC3T3-E1 preosteoblast cells were exposed to Dex.

A growing number of studies have underlined the pivotal roles of TRIM21 in tumorigenesis (26), immune response (5) and autophagy (27). TRIM21 is downregulated during the osteogenic

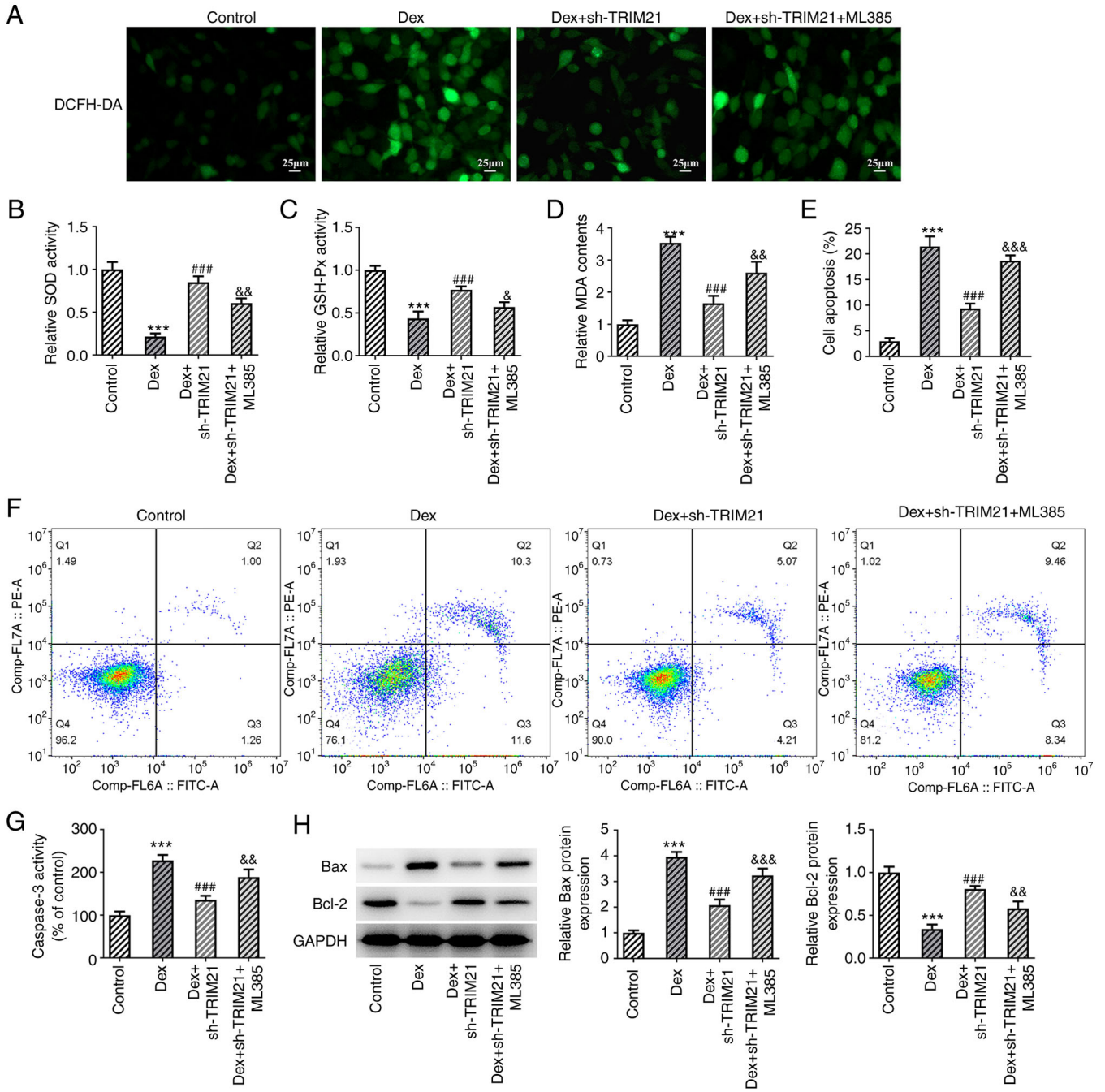

Figure 5. TRIM21 deletion activates Kelch-like ECH-associated protein 1/nuclear factor erythroid 2-related factor 2 signaling to hamper oxidative stress and apoptosis in Dex-treated MC3T3-E1 cells. (A) DCFH-DA staining evaluated reactive oxygen species generation. The levels of (B) SOD, (C) GSH-Px and (D) MDA were detected by the corresponding kits. (E and F) Flow cytometry analysis of cell apoptosis. (G) Caspase 3 activity as measured by a kit. (H) Western blotting of apoptosis-associated proteins. ***P<0.001 vs. control group; $^{###}$P<0.001 vs. Dex group; $^{&}$P<0.05, $^{&&}$P<0.01, $^{&&&}$P<0.001 vs. Dex + sh-TRIM21 group. TRIM21, tripartite motif-containing protein 21; Dex, dexamethasone; DCFH-DA, 2,7-dichloro-dihydrofluorescein diacetate; SOD, superoxide dismutase; GSH-Px, glutathione peroxidase; MDA, malonaldehyde; sh-, short hairpin RNA; sh-TRIM21, sh-RNA targeting TRIM21.

process of mesenchymal stem cells (8). In addition, Liu *et al* (28) demonstrated that TRIM21 expression is elevated in bone specimens from osteoporosis patients and ovariectomy-induced osteoporotic mice. Their findings also supported the hypothesis that TRIM21 depletion promotes bone formation by enhancing the osteogenic differentiation of bone marrow mesenchymal stem cells and elevating the activity of osteoblast. In the present study, TRIM21 expression was raised in MC3T3-E1 cells challenged with Dex and the viability loss and LDH release in Dex-treated MC3T3-E1 cells were both reversed by silencing of TRIM21. Additionally, enhanced osteoblast apoptosis has been documented to play a crucial role in the development and maintenance of bones and to further the progression of glucocorticoids-induced ONFH (29,30). By contrast, in Dex-exposed MC3T3-E1 cells, knockdown of TRIM21 attenuated the apoptotic ability of MC3T3-E1 cells, reduced caspase 3 activity and pro-apoptotic Bax expression and enhanced anti-apoptotic Bcl-2 expression. Comparing the results of cell activity and apoptosis of Dex-treated MC3T3-E1, it was found that the cell viability of Dex and Dex + shNC groups was ~50%, but the cell apoptosis rate in that two

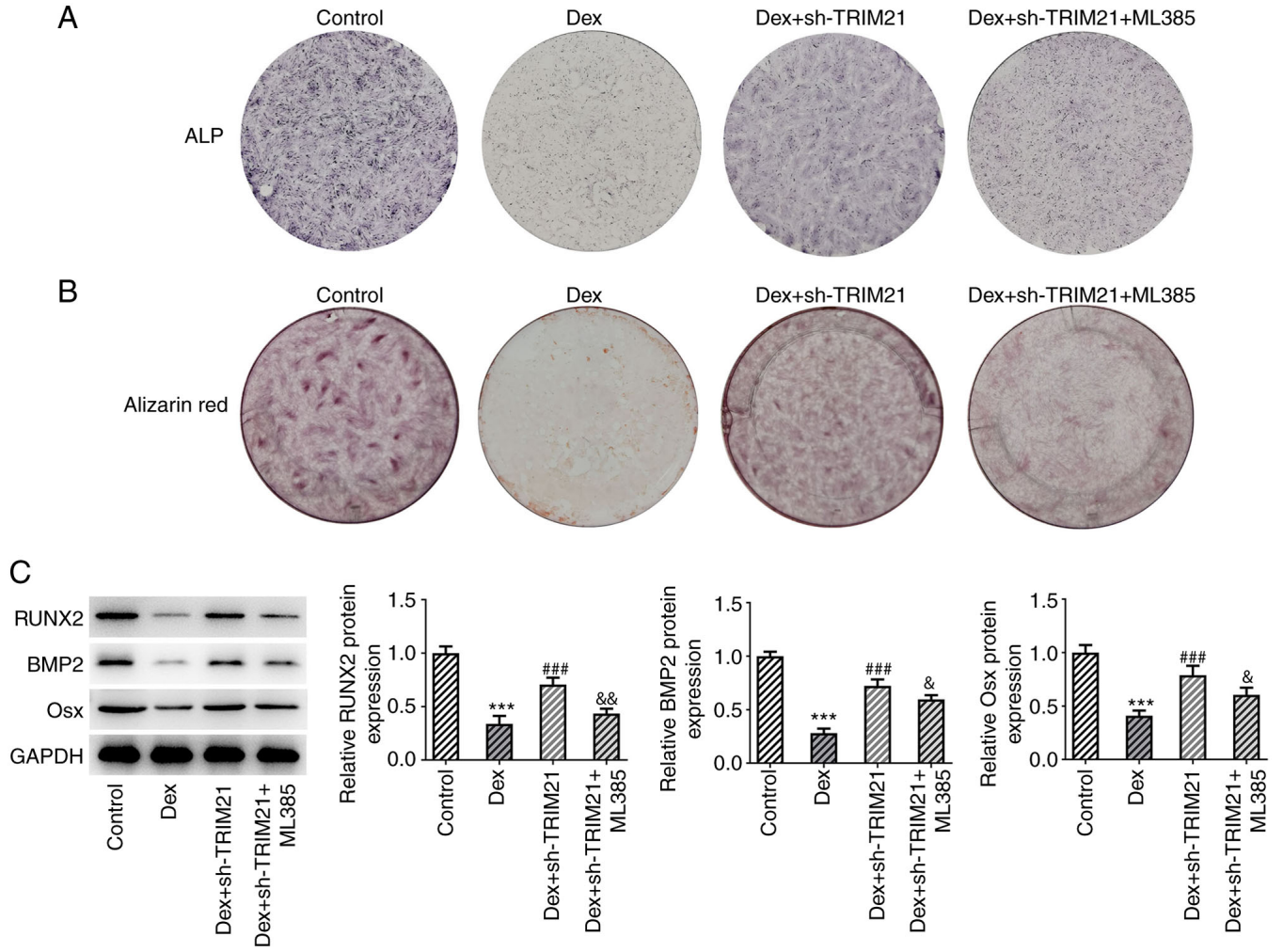

Figure 6. TRIM21 depletion activates Keap1/Nrf2 signaling to drive the osteogenic differentiation in Dex-treated MC3T3-E1 cells. (A) ALP staining measured ALP activity. (B) Alizarin red S staining estimated calcium salt deposition. (C) Western blotting tested the expression of osteogenic differentiation-associated proteins. ***P<0.001 vs. control group; $^{\#\#\#}$P<0.001 vs. Dex group; $^{\&}$P<0.05, $^{\&\&}$P<0.01 vs. Dex + sh-TRIM21 group. TRIM21, tripartite motif-containing protein 21; Keap1, Kelch-like ECH-associated protein 1; Nrf2, nuclear factor erythroid 2-related factor 2; Dex, dexamethasone; ALP, alkaline phosphatase; sh-, short hairpin RNA; sh-TRIM21, sh-RNA targeting TRIM21; RUNX2, runt-related transcription factor 2; BMP2, bone morphogenetic protein 2; Osx, osterix.

groups was only ~20%. The reason for this result may be that there are other forms of cell death involved in this process, such as necrosis and ferroptosis (31,32). Oxidative stress, resulting in ROS accumulation, is the leading cause of osteoblast injury and death (33). Altered ROS generation can facilitate osteoblast apoptosis and deplete the expression of antioxidant enzymes leading to ONFH (34). Meanwhile, TRIM21 reduction has been reported to inactivate oxidative stress in intervertebral disc degeneration (35) and atrial remodeling (36). Consistent with this, the present study showed that TRIM21 knockdown decreased Dex-induced ROS production, decreased SOD and GSH-Px activities and increased MDA activity in MC3T3-E1 cells.

Osteogenic differentiation is deemed a pivotal determinant in bone regeneration (37). Abnormal bone remodeling and osteoblastic bone formation have been shown to participate in the occurrence and progression of ONFH (38). Belonging to the BMP family, BMP2, which plays a major role in bone development and remodeling, is a well-established promoter of osteoblastic differentiation and bone formation (39). Runx2 is the main downstream regulator of the BMP signaling pathway that regulates the expression of several osteogenic genes (40). Osx is indispensable for osteogenic differentiation and its overexpression is related to the enhancement of osteogenic differentiation (41). Notably, the absence of TRIM21 may potentiate osteogenic differentiation and decrease RUNX2 expression in mesenchymal stem cells (8). In the current study, after TRIM21 was knocked down in MC3T3-E1 cells challenged with Dex, the ALP activity was increased, calcium salt deposition was strengthened and Osx, RUNX2 and BMP2 protein expressions were all increased.

Furthermore, an emerging study has underlined that TRIM21 may serve an inhibitor role in Keap1/Nrf2 signaling in hepatocarcinogenesis (13). Nrf2, a member of the Cap-n-Collar family of basic leucine zipper proteins, is regarded as a major anti-oxidative modulator by contributing to the transcription of antioxidant genes (42). As a main repressor protein of Nrf2, Keap1 facilitates the polyubiquitination of the Nrf2 protein and drives proteasome-dependent Nrf2 degradation (42). Under unstressed conditions, Keap1 binds to Nrf2 and promotes its degradation. Once the cells are damaged, Nrf2 will dissociate

from Keap1, translocate into the nucleus and subsequently activate various genes, including HO-1 (42). Abundant evidence has demonstrated that activation of Keap1/Nrf2 signaling can mitigate oxidative stress in the process of steroid-induced ONFH (18). Li *et al* (43) showed that the Nrf2 knockdown exacerbates apoptosis, oxidative stress and inflammation while inhibiting the osteogenic differentiation of high glucose-stimulated MC3T3-E1 cells. The present data also demonstrated that Nrf2 inhibitor ML385 partially counteracted the effects of TRIM21 deletion on apoptosis, oxidative stress as well as osteogenic differentiation in Dex-treated MC3T3-E1 cells.

Collectively, the present study showed that TRIM21 interference activated the Keap1/Nrf2 pathway to antagonize Dex-triggered apoptosis, oxidative stress and osteogenic differentiation decrease in MC3T3-E1 cells, thereby relieving the progression of steroid-induced ONFH. All these outcomes emphasize that TRIM21 may be valued as a potential target for steroid-induced ONFH. Nevertheless, this study only explored the effect of TRIM21 on mouse preosteoblast cells. Further experiments associated with osteoclast will be analyzed in the future. In addition, the other signaling pathways downstream of TRIM21, such as the YAP1/β-catenin signaling pathway (28), the intervention timing and possible screening models for high-risk patients will also be investigated in the next studies.

Acknowledgements

Not applicable.

Funding

No funding was received.

Availability of data and materials

The data generated in the present study may be requested from the corresponding author.

Authors' contributions

JS and XM conceived and designed the study. JS, LC, XW and XM conducted the experiments. LC and XW performed the literature search and data extraction. JS drafted the manuscript and XM revised it. All authors read and approved the final version of the manuscript. JS and XM confirm the authenticity of all the raw data.

Ethics approval and consent to participate

Not applicable.

Patient consent for publication

Not applicable.

Competing interests

The authors declare that they have no competing interests.

References

1. Pan J, Lu L, Wang X, Liu D, Tian J, Liu H, Zhang M, Xu F and An F: AIM2 regulates vascular smooth muscle cell migration in atherosclerosis. Biochem Biophys Res Commun 497: 401-409, 2018.
2. Hines JT, Jo WL, Cui Q, Mont MA, Koo KH, Cheng EY, Goodman SB, Ha YC, Hernigou P, Jones LC, *et al*: Osteonecrosis of the femoral head: An updated review of ARCO on pathogenesis, staging and treatment. J Korean Med Sci 36: e177, 2021.
3. Ando W, Sakai T, Fukushima W, Kaneuji A, Ueshima K, Yamasaki T, Yamamoto T and Nishii T; Working group for ONFH guidelines and Sugano N: Japanese orthopaedic association 2019 guidelines for osteonecrosis of the femoral head. J Orthop Sci 26: 46-68, 2021.
4. Watanabe M and Hatakeyama S: TRIM proteins and diseases. J Biochem 161: 135-144, 2017.
5. Jones EL, Laidlaw SM and Dustin LB: TRIM21/Ro52-roles in innate immunity and autoimmune disease. Front Immunol 12: 738473, 2021.
6. Ben-Chetrit E, Chan EK, Sullivan KF and Tan EM: A 52-kD protein is a novel component of the SS-A/Ro antigenic particle. J Exp Med 167: 1560-1571, 1988.
7. Ben-Chetrit E, Fox RI and Tan EM: Dissociation of immune responses to the SS-A (Ro) 52 and 60-kd polypeptides in systemic lupus erythematosus and Sjögren's syndrome. Arthritis Rheum 33: 349-355, 1990.
8. Xian J, Liang D, Zhao C, Chen Y and Zhu Q: TRIM21 inhibits the osteogenic differentiation of mesenchymal stem cells by facilitating K48 ubiquitination-mediated degradation of Akt. Exp Cell Res 412: 113034, 2022.
9. Ulasov AV, Rosenkranz AA, Georgiev GP and Sobolev AS: Nrf2/Keap1/ARE signaling: Towards specific regulation. Life Sci 291: 120111, 2022.
10. Fan Z, Wirth AK, Chen D, Wruck CJ, Rauh M, Buchfelder M and Savaskan N: Nrf2-Keap1 pathway promotes cell proliferation and diminishes ferroptosis. Oncogenesis 6: e371, 2017.
11. Song MY, Lee DY, Chun KS and Kim EH: The role of NRF2/KEAP1 signaling pathway in cancer metabolism. Int J Mol Sci 22: 4376, 2021.
12. Yang N, Sun H, Xue Y, Zhang W, Wang H, Tao H, Liang X, Li M, Xu Y, Chen L, *et al*: Inhibition of MAGL activates the Keap1/Nrf2 pathway to attenuate glucocorticoid-induced osteonecrosis of the femoral head. Clin Transl Med 11: e447, 2021.
13. Wang F, Zhang Y, Shen J, Yang B, Dai W, Yan J, Maimouni S, Daguplo HQ, Coppola S, Gao Y, *et al*: The ubiquitin E3 ligase TRIM21 promotes hepatocarcinogenesis by suppressing the p62-Keap1-Nrf2 antioxidant pathway. Cell Mol Gastroenterol Hepatol 11: 1369-1385, 2021.
14. Han D, Gu X, Gao J, Wang Z, Liu G, Barkema HW and Han B: Chlorogenic acid promotes the Nrf2/HO-1 anti-oxidative pathway by activating $p21^{Waf1/Cip1}$ to resist dexamethasone-induced apoptosis in osteoblastic cells. Free Radic Biol Med 137: 1-12, 2019.
15. Hu Q, Zuo T, Deng L, Chen S, Yu W, Liu S, Liu J, Wang X, Fan X and Dong Z: β-Caryophyllene suppresses ferroptosis induced by cerebral ischemia reperfusion via activation of the NRF2/HO-1 signaling pathway in MCAO/R rats. Phytomedicine 102: 154112, 2022.
16. Livak KJ and Schmittgen TD: Analysis of relative gene expression data using real-time quantitative PCR and the 2(-Delta Delta C(T)) method. Methods 25: 402-408, 2001.
17. Suzuki T, Takahashi J and Yamamoto M: Molecular basis of the KEAP1-NRF2 signaling pathway. Mol Cells 46: 133-141, 2023.
18. Lu Z and Han K: SMAD4 transcriptionally activates GCN5 to inhibit apoptosis and promote osteogenic differentiation in dexamethasone-induced human bone marrow mesenchymal stem cells. Steroids 179: 108969, 2022.
19. Palekar G: Hip preservation with autologous osteoblast cell-based treatment in osteonecrosis of the femoral head. Orthopedics 44: e183-e189, 2021.
20. Kerachian MA, Séguin C and Harvey EJ: Glucocorticoids in osteonecrosis of the femoral head: A new understanding of the mechanisms of action. J Steroid Biochem Mol Biol 114: 121-128, 2009.
21. Fang L, Zhang G, Wu Y, Li Z, Gao S and Zhou L: SIRT6 prevents glucocorticoid-induced osteonecrosis of the femoral head in rats. Oxid Med Cell Longev 2022: 6360133, 2022.

22. Sun F, Zhou JL, Wei SX, Jiang ZW and Peng H: Glucocorticoids induce osteonecrosis of the femoral head in rats via PI3K/AKT/FOXO1 signaling pathway. PeerJ 10: e13319, 2022.
23. Peng P, Nie Z, Sun F and Peng H: Glucocorticoids induce femoral head necrosis in rats through the ROS/JNK/c-Jun pathway. FEBS Open Bio 11: 312-321, 2021.
24. Deng S, Dai G, Chen S, Nie Z, Zhou J, Fang H and Peng H: Dexamethasone induces osteoblast apoptosis through ROS-PI3K/AKT/GSK3β signaling pathway. Biomed Pharmacother 110: 602-608, 2019.
25. Zhou M, Liu L, Xu Y, Jiang J, Liu G and Zhai C: Effects of osteoblast autophagy on glucocorticoid-induced femoral head necrosis. Jt Dis Relat Surg 31: 411-418, 2020.
26. Alomari M: TRIM21-a potential novel therapeutic target in cancer. Pharmacol Res 165: 105443, 2021.
27. Kimura T, Jain A, Choi SW, Mandell MA, Schroder K, Johansen T and Deretic V: TRIM-mediated precision autophagy targets cytoplasmic regulators of innate immunity. J Cell Biol 210: 973-989, 2015.
28. Liu RX, Gu RH, Li ZP, Hao ZQ, Hu QX, Li ZY, Wang XG, Tang W, Wang XH, Zeng YK, *et al*: Trim21 depletion alleviates bone loss in osteoporosis via activation of YAP1/β-catenin signaling. Bone Res 11: 56, 2023.
29. Nie Z, Chen S and Peng H: Glucocorticoid induces osteonecrosis of the femoral head in rats through GSK3β-mediated osteoblast apoptosis. Biochem. Biophys Res Commun 511: 693-699, 2019.
30. Mutijima E, De Maertelaer V, Deprez M, Malaise M and Hauzeur JP: The apoptosis of osteoblasts and osteocytes in femoral head osteonecrosis: Its specificity and its distribution. Clin Rheumatol 33: 1791-1795, 2014.
31. Guo S, Mao L, Ji F, Wang S, Xie Y, Fei H and Wang XD: Activating AMP-activated protein kinase by an α1 selective activator compound 13 attenuates dexamethasone-induced osteoblast cell death. Biochem Biophys Res Commun 471: 545-552, 2016.
32. Sun F, Zhou JL, Liu ZL, Jiang ZW and Peng H: Dexamethasone induces ferroptosis via P53/SLC7A11/GPX4 pathway in glucocorticoid-induced osteonecrosis of the femoral head. Biochem Biophys Res Commun 602: 149-155, 2022.
33. Yang YH, Li B, Zheng XF, Chen JW, Chen K, Jiang SD and Jiang LS: Oxidative damage to osteoblasts can be alleviated by early autophagy through the endoplasmic reticulum stress pathway-implications for the treatment of osteoporosis. Free Radic Biol Med 77: 10-20, 2014.
34. Deng S, Zhou JL, Fang HS, Nie ZG, Chen S and Peng H: Sesamin protects the femoral head from osteonecrosis by inhibiting ROS-induced osteoblast apoptosis in rat model. Front Physiol 9: 1787, 2018.
35. Zheng J, Chang L, Bao X, Zhang X, Li C and Deng L: TRIM21 drives intervertebral disc degeneration induced by oxidative stress via mediating HIF-1α degradation. Biochem Biophys Res Commun 555: 46-53, 2021.
36. Liu X, Zhang W, Luo J, Shi W, Zhang X, Li Z, Qin X, Liu B and Wei Y: TRIM21 deficiency protects against atrial inflammation and remodeling post myocardial infarction by attenuating oxidative stress. Redox Biol 62: 102679, 2023.
37. Bharadwaz A and Jayasuriya AC: Osteogenic differentiation cues of the bone morphogenetic protein-9 (BMP-9) and its recent advances in bone tissue regeneration. Mater Sci Eng C Mater Biol Appl 120: 111748, 2021.
38. Tingart M, Beckmann J, Opolka A, Matsuura M, Wiech O, Grifka J and Grässel S: Influence of factors regulating bone formation and remodeling on bone quality in osteonecrosis of the femoral head. Calcif Tissue Int 82: 300-308, 2008.
39. Halloran D, Durbano HW and Nohe A: Bone morphogenetic protein-2 in development and bone homeostasis. J Dev Biol 8: 19, 2020.
40. Liu DD, Zhang CY, Liu Y, Li J, Wang YX and Zheng SG: RUNX2 regulates osteoblast differentiation via the BMP4 signaling pathway. J Dent Res 101: 1227-1237, 2022.
41. Han Y, Kim YM, Kim HS and Lee KY: Melatonin promotes osteoblast differentiation by regulating osterix protein stability and expression. Sci Rep 7: 5716, 2017.
42. Baird L and Yamamoto M: The molecular mechanisms regulating the KEAP1-NRF2 pathway. Mol Cell Biol 40: e00099-20, 2020.
43. Li X, Yu X, He S and Li J: Dipeptidyl peptidase 3 is essential for maintaining osteoblastic differentiation under a high-glucose environment by inhibiting apoptosis, oxidative stress and inflammation through the modulation of the Keap1-Nrf2 pathway. Int Immunopharmacol 120: 110404, 2023.